J Mater Sci: Mater Med (2008) 19:189–195
DOI 10.1007/s10856-006-0101-2

Physical characterization of polycaprolactone scaffolds

Jorge Más Estellés · Ana Vidaurre · José M. Meseguer Dueñas · Isabel Castilla Cortázar

Received: 8 May 2006 / Accepted: 4 December 2006 / Published online: 28 June 2007

Abstract Films and sponges were prepared from a solution of Poly(ε-caprolactone) (PCL) in tetrahydrofuran (THF). The porosity, crystallinity, and mechanical properties of the samples were studied. Porosity of around 15% was obtained for the films produced by evaporation of THF at room temperature. A much more porous structure (50–70%) was found for the sponges obtained by cooling the solution at –30 °C and subsequently eliminating the solvent by freeze drying. The porosity of the samples was also observed by scanning electron microscopy (SEM). The crystallinity of the samples was studied by the calorimetric technique (DSC) before and after the compression scans. The mechanical properties of the different samples were determined by compression test, and were compared to those corresponding to the PCL in bulk. The compression scans did not affect the crystallinity of the samples. The variations observed in the results of the different scans were attributed to the differences in porosities and crystallinity.

Introduction

Poly(ε-caprolactone) (PCL) is a biocompatible and semicrystalline polymer, proposed for a wide variety of biomedical applications. It is a biodegradable polymer having a melting point T_m of ~60 °C and a glass transition temperature (T_g) of ~–60 °C [1]. At present, it is regarded as a soft and hard-tissue compatible material for biomedical applications, including resorbable sutures, drug delivery systems [2–5], and scaffold for tissue engineering [6–10]. Its low rate of hydrolytic degradation [11, 12] makes this polymer useful for long term applications [13, 14]. PCL has previously been shown to support cell attachment and proliferation and has been investigated as matrix material for cell culture: fibroblast [9, 15], osteoblast [16], chondrogenesis of messenchymal stem cells [17], for craniofacial reconstruction [18, 19] and nerve guides [20].

Several techniques, such as porogen leaching [21–23] foaming [24], fiber processing [25], microfabrication technique PAM (pressure-activated microsyringe) [26], gravity spun [15] and 3D microprinting [27] have been developed to produce polymer porous scaffolds for tissue engineering, many of which yield different porous structures with varying degrees of porosity, different pore size, pore shape and interconnection between pores, as well as different mechanical properties of the scaffolds. Phase separation is a common technique used to fabricate porous scaffold with interconnective pores [28]. Surface properties play an important role in cell adhesion and proliferation. Tang et al. [29] have studied the effect of surface topography on the ability of fibroblast to adhere and proliferate on a film surface. The mechanical strength and stiffness should ideally approach those of the tissue it is to replace while maintaining an interconnected pore network for cell migration and nutrient transport [27]. These requirements result in conflicting design goals. Hollister et al. [30] have developed an image-based optimization scheme for the design and fabrication of scaffolds. If the seeded polymer is biodegradable, once introduced into a patient it will gradually

J. Más Estellés · A. Vidaurre (✉) · J. M. Meseguer Dueñas · I. Castilla Cortázar
Department of Applied Physics, Center for Biomaterials, Universidad Politécnica de Valencia, Camino de Vera s/n, Valencia 46071, Spain
e-mail: vidaurre@fis.upv.es

resorb, leaving behind a matrix of connective tissue and cells with the appropriate structural and mechanical properties [31].

In this work, two series of film and sponge PCL samples were prepared by the phase separation method. Both type of sample show very different morphology, porosity and mechanical properties. Four consecutive compression scans were performed on each sample. The mechanical results obtained were correlated with the porosity and crystallinity of the samples.

Experimental

Materials

Poly(caprolactone) [Polysciences (M_w 43,000–50,000)] in the form of pellets was used without further purification. The solvent, tetrahydrofuran from Aldrich (THF), was used as received.

Preparation of PCL samples

The PCL film was produced by using a solvent casting technique. Around 6 g of PCL pellets were dissolved in 54, 24, 14 g of THF, obtaining solutions with concentrations of 10%, 20% and 30% w/w, respectively. For concentrations higher than 10%, the solution was warmed in an oven at 38 °C to aid in dissolving the pellets. The solution was poured into a glass Petri dish (diameter 90 mm), which was covered with a lid (diameter 100 mm) and placed in a fume hood at room temperature for slow evaporation. The solid samples were dried in vacuum to constant weight. The film samples obtained presented a flat white surface. The thickness of the resulting films ranged from 0.9 mm to 1.2 mm.

The sponges were obtained by the liquid phase separation method. Different amounts of PCL pellets were dissolved in THF to get approximately 15 g of homogeneous solutions at concentrations of 10%, 20%, 30%, 40% w/w. The solution was poured into a test tube that was immersed in a bath at –30 °C for about 2 h, the time required for the solution to become viscous. The test tube was then connected to a vacuum pump (Packtel, Alcatel) at a pressure of 10^{-4} bar to allow the THF solvent to evaporate, while maintaining the frozen porous structure. Depending on the amount of solvent, this process took between 8 h and 20 h. A white, uniform, cylindrical material was obtained (visual assessment). The samples prepared from the 10% solution tended to fragment easily on handling. The sponges prepared from the 20%, 30%, and 40% solutions were consistent and could be cut into slices for subsequent measurements.

For the sake of comparison, bulk samples were obtained by melting the PCL pellets onto glass plates to get a film of approximately 0.8 mm thick

Characterization

Morphology and porosity

The samples were fractured in liquid nitrogen using a razor blade and then sputter coated with gold. The morphology of the porous samples was observed with JEOL JSM-5410 microscope equipped with an Oxford CT 1,500 cryounit.

The porosity of samples, φ, was estimated from the apparent volume, V_T, and the PCL volume V_M defined from the actual amount of polymer, m, and its mean density, ρ(ρ = 1.14 g/cm^3)

$$\phi = \frac{V_T - V_M}{V_T} = \frac{V_T - \frac{m}{\rho}}{V_T}$$

The porosity was evaluated for the whole samples (100 mm diameter disk for the film samples, and cylinders of around 1 cm diameter, and 10 cm length for the sponges).

Differential scanning calorimetry (DSC) measurements

Melting temperature of the samples was measured by using a Pirys (Perkin Elmer) DSC calibrated with indium. The measurements were carried out at a scan rate of 10 °C/min between –40 °C and 120 °C. The weight of the samples was around 15 mg for all the samples except for the DSC measurements of the samples submitted to the compression test, which were around 5 mg. The melting point was determined at the maximum of the melting endotherm. Crystallinity was calculated assuming proportionality to the experimental heat of fusion using the reported heat of fusion of 139.5 J/g for the 100% crystalline PCL [11]. After this heating scan the sample was cooled down to –40 °C at a rate of –10 °C/min and reheated again to 120 °C at a rate of 10 °C/min. The data of all three scans were collected for subsequent analysis.

Mechanical test

The mechanical properties were measured using a Microtest machine 15 N load cell and a crosshead speed of 1 μm/s. The uncertainties were 0.01 N for the force and 0.001 mm for the displacement. In the case of film and bulk samples, the specimens were cylindrical (2.25 mm in diameter and the thickness corresponding to each sample). The sponge samples presented difficulties for cutting into regular slabs. Two parallel cuts were

Table 1 Porosity of the sponge samples

Sponges: PCL/THF (%)	Porosity (±10%)
40	50
30	60
20	70
10	–

made and the cross section was measured by image analysis, obtaining values between 15 mm^2 and 20 mm^2. The compressive modulus was calculated as the slope of the linear portion of the stress-strain curve in the range between 2 MPa and 3 MPa, with an estimated uncertainty of ±3 MPa. The value of the initial length was that corresponding to the initial length of each scan. To examine the elastic recovery, four consecutive scans were performed. Each scan went from a position in which there was no contact between the upper plate and the sample to a position in which the load force was 15 N. Data on the position of the mobile plate and the load force were collected every second. During the four consecutive scans the sample was not subjected to manipulation. The initial length of the sample in each scan was determined by the position in which the same force was detected like during the first scan. The plastic deformation was defined as the difference between the initial length of the sample and the length at the beginning of the scan i-th: $\Delta l = l_0 - l_{0i}$.

Results

Morphology and porosity

The estimation of porosity gave values around 15% for all the film samples, whatever the initial concentration of the solution. SEM microphotographs (not shown) presented differences in the morphology of the samples depending on concentration, though this had no influence on porosity. The solution concentration had greater importance in the case of the sponges. At –30 °C the solution became so viscous that the structure was maintained during the solvent extraction. As shown in Table 1, the porosity increased with increasing amounts of solvent (in fact, it was proportional to the amount of THF); the measured porosity was 50% for the sample obtained from the 40% PCL/THF solution, 60% for the 30%, and 70% for 20% PCL/THF solution. In the sample from the 10% PCL/THF solution, it was not possible to determine the apparent volume of the sample since it converted to powder. As we have said, the measurements were performed for the whole sample; when small portions were measured, differences in porosity were found. The estimated uncertainty calculated from the standard deviation of 5 measurements is of the order of 10%.

Figure 1a–c shows SEM microphotographs of the PCL sponges obtained from the 10%, 20%, and 30% PCL/THF solution; in all cases the resulting morphology was similar, with changes in the size of the micro-spheres and their connectivity. The size of the micro-spheres decreases with the PCL concentration, ranging from 150 μm average-

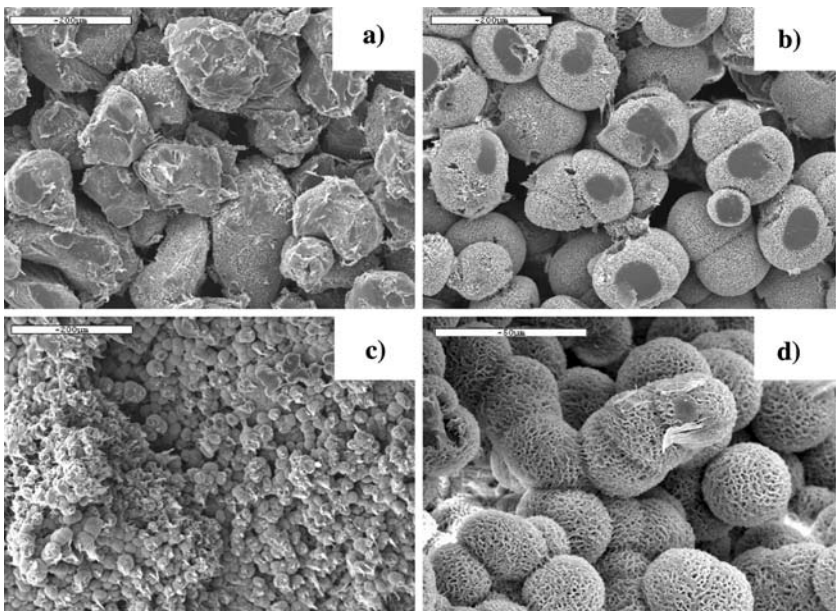

Fig. 1 SEM microphotographs of the PCL sponges, (**a**) obtained from the 10% solution in THF, (**b**) from the 20% solution, and (**c**) from the 30% solution. (**d**) Spheres surface morphology of the 30% sponge

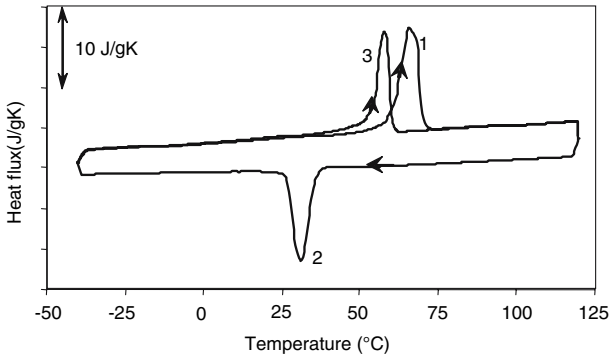

Fig. 2 DSC thermograms for PCL film obtained from the 10% solution in THF

diameter in the case of 10% sponge to 30 μm in the 30% sponge. While the 10% sponge is made of isolated spheres, they became interconnected when the PCL proportion increases, giving rise to a more compact structure. The spheres present a porous microstructure (Fig. 1d) of around 5 μm in size.

Thermal properties

The melting point obtained for the bulk PCL sample is of the same order as that reported in the literature (59.1 ± 0.5) °C [32]; the position and area of the melting peak in the second heating scan is the same as in the first. The results for the film and sponge samples are similar to those given in Fig. 2. The melting temperature measured in the first scan (number 1) is always higher than that obtained in the second heating scan (number 3), after crystallization. The position and area of the second heating scan measured in the film and sponge samples are similar to that corresponding to the bulk sample.

Table 2 shows the results of melting temperature and crystallinity for the three kinds of samples. Those prepared from the PCL solution in THF present a greater crystallinity than the bulk samples. Sponges and films prepared from PCL/THF solutions of different concentrations present similar melting temperature values. The crystallinity in the film samples decreases when there is an increase in the concentration of PCL in the PCL/THF solution. On the other hand, the crystallinity of the sponges increases with the PCL concentration.

The crystallinity was also measured after the compression scans. The results obtained were of the same order as the corresponding values before the compression test. The estimated error is 3%, due to the smaller size of the samples.

Mechanical properties

Figures 3–5 show the stress-strain curves obtained for the bulk sample, the film sample obtained from the 10% PCL/THF solution and the sponge from the 40% PCL/THF solution. The results obtained for the film samples are similar to those shown in Fig. 4 and the results corresponding to the sponge from the 30% PCL/THF solution are similar to those shown in Fig. 5. Sponges made from solutions with 10% and 20% concentrations tended to fragment when handled and it was therefore impossible to perform a compression test on these samples.

In all the measurements corresponding to bulk and film samples, some general features can be observed: (a) the curve presents two linear regions with a transition zone between them; (b) the unitary deformation at the end of the first scan is always greater than that corresponding to the same stress in the successive scans; (c) the results for these posterior scans are very similar for each sample. These two last features can also be observed in the sponge measurements. Table 2 shows the results obtained for the maximum deformation in the first and fourth scans.

The length measured at the beginning of each scan gives us the measurement of the length recovery in the preceding

Table 2 Melting point, degree of crystallization, maximum strain and Young's modulus measured in the first and fourth compression scans, and plastic deformation after first scan for the different types of sample

Sample	(T_m ± 0.5)°C	(χ ± 1) (%)	Max. strain first scan (%) (±1)	Max. strain fourth scan (%) (±1)	Young's modulus first scan (MPa) (±3)	Young's modulus fourth scan (MPa) (±3)	Plastic deformation after first scan (%) (±1)
Bulk	59.1	61	18	12	34	68	6
10% Film	66.1	69.1	9	6	72	95	4
20% Film	66.4	67	21	10	43	90	12
30% Film	66.4	66	22	10	33	85	10
20% Sponge	64.5	69.7	–	–	–	–	–
30% Sponge	62.4	76.4	50	10	–	13	50
40% Sponge	64.4	76.9	52	14	–	13	46

The percentage represents the PCL concentration in the PCL/THF solution

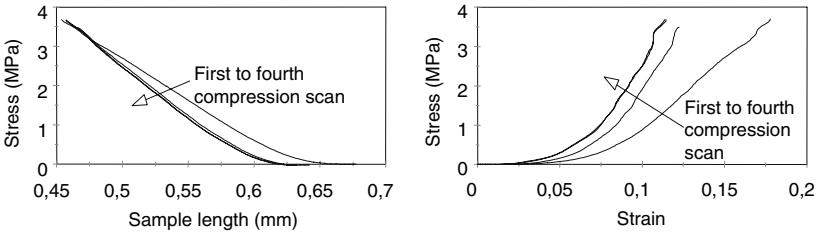

Fig. 3 Stress curves for the bulk sample, as a function of the sample length (left), as a function of the unit strain (right)

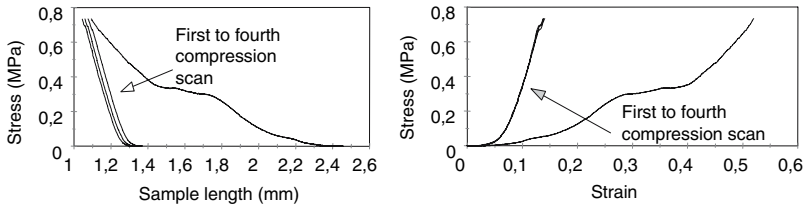

Fig. 5 Stress curves for the sponge obtained from the 40% PCL solution, as a function of the sample length (left), as a function of the unit strain (right)

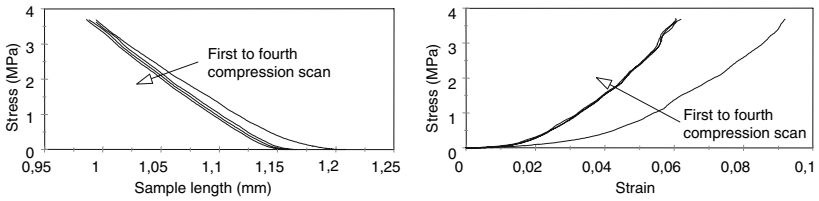

Fig. 4 Stress curves for the film sample obtained from the 10% PCL solution, as a function of the sample length (left), as a function of the unit strain (right)

scan. There is a change between the initial length and the length measured after the first scan, but there is no change after the second and third scans, in comparison with the length after the first scan. This length change can be seen in Table 2. As the measurements were carried out at room temperature around 20 °C (80 °C above glass transition temperature), no subsequent relaxation could be expected.

The compressive moduli for the bulk and film samples were calculated as the slope of the linear portion of the stress-strain curve in the range between 2 MPa and 3 MPa. Two values were calculated for each sample, corresponding to the first and the fourth scan. The value of the initial length is considered as that corresponding to each scan. The results for Young's modulus are shown in Table 2.

The results for the stress-strain curve corresponding to the 40% sponges shown in Fig. 5 are qualitatively different from the bulk and film results (Figs. 3 and 4 respectively). The cross section of the sponges was greater than that corresponding to bulk and film samples, giving rise to a lower maximum stress for the same load. The curve presents a plateau zone, corresponding to the collapse of the elastoplastic pores [33]. The compressive modulus corresponding to the fourth scan was calculated as the slope of the linear portion in the range between 0.4 MPa and 0.6 MPa. As the compressive modulus for the sponges were calculated in a different stress range than the bulk and film samples, they are not comparable. We did not obtain the compression moduli for the first scan due to the plateau of the curves.

Discussion

The higher crystallinity of the film and sponges samples obtained from the THF solution, compared to the bulk sample, can be explained by the rearrangement of the chains in the solution. Concerning the film samples, nucleation and growth of the crystalline phase occurs throughout the THF evaporation process. As the THF evaporates, the viscosity of the solution increases and therefore the mobility of the PCL chains diminish. As shown in Table 2, the crystallinity decreases when increasing the initial PCL concentration in the solution, as would be expected from the fact that the PCL chains have less mobility and less time to organize the crystalline structure. At a constant temperature, the crystallization process depends on the PCL concentration, which changes from the initial concentration to 100% when all the solvent evaporates. On the other hand, although sponges were also obtained from the TFH solution, it became a viscous fluid when the temperature decreased. The nucleation and growth of the crystalline phase takes place in the first step when the sample is quenched to –30 °C and the presence of the solvent allows the rearrangement of the PCL chains

and, in this case, higher concentration in the PCL/THF solution produces higher crystallinity. At the low concentration limit, the PCL molecules are dispersed and their low mobility does not facilitate the crystallization process. Phase separation produces independent spheres with a lower degree of crystallization. When the PCL concentration is higher, highly crystalline interconnected spheres can be produced.

According to the 4th scan results, there is a correlation between Young's modulus and crystallinity in all the film samples (Table 2), as expected [34]. The higher crystallinity of the films versus the bulk samples causes its greatest Young's modulus, measured in the fourth scan. As we have said above, we can not compare the sponge samples' moduli with the film and bulk samples since they were calculated in different stress ranges.

There is a plastic deformation between the first and the successive scans in all the samples studied (Table 2) that could be explained both by the semicrystalline characteristic of PCL and by the porosity of the samples.

The corresponding differences between the first and second compression scans observed in all the film samples can be explained as an effect of the densification produced by the collapse of the pores, due to elastoplastic deformation; densification also produces a rise in the measured Young's modulus (see Table 2). The whole plastic deformation is produced in the first scan, which explains why the second to fourth scans are very similar. To understand what happens in the successive compression scans let us focus our attention on the 10% PCL film sample (Fig. 4 and Table 2). The plastic deformation after the first scan is 4%, and the measured porosity 15%, which means that only 4/15 of the pore collapse corresponds to plastic deformation, while the other 11/15 of the deformation (elastic deformation) is recoverable.

In the case of the bulk samples (non-porous samples) the plastic deformation is of 6% (Table 2) and a possible explanation for this behavior would be to assume a lateral expansion of the sample, which involves a diameter augmentation from 2.25 mm to 2.32 mm. This change in the diameter is very small and therefore not possible to measure. This assumption could justify the whole plastic deformation, which affects only the amorphous phase of the sample, that is above the glass transition temperature (T_g) and therefore in the rubber-like state. As a consequence, in successive scans the rise in Young's modulus (34–68 MPa) should be due to the performance of the crystalline phase.

One would therefore not expect plastic lateral expansion of the film samples when the pores are not yet collapsed (the maximum strain in the first scan for the 10% film sample is 9% and the estimated porosity was around 15%). Thus, when the sample is under compression the pores are being "squashed", with a constant cross section of the sample. However, in the 20% and 30% PCL film samples, the plastic deformation was 12% and 10%, respectively, its Young's modulus measured in the first scan being lower than that corresponding to the 10% film sample. This could be correlated with the different crystallinity (Table 2) and the porosity of the samples [33] and would mean that the porosity of the sample from the 10% solution should be lower than the porosity of the samples obtained from the 20% and 30% solutions. This result seems to contradict the estimation of the porosity obtained from the measurement of the apparent volume, which gives the same value for all the film samples. But it is necessary to take into account the fact that samples may not be homogeneous. As we have said above, the porosity calculated from the apparent volume is the mean porosity of the whole sample, while the results obtained from the compression measurements are calculated for a small portion of the sample (2.25 mm disk).

In the case of sponge samples, the main feature is the presence of a plateau zone, corresponding to the elastoplastic collapse of the pores. The 40% PCL sponge in Fig. 5 suffers a 46% plastic deformation (Table 2), very close to the porosity measured 50% (Table 1). This would mean that, in this type of sample, all the pore collapse is unrecoverable. A similar result is obtained for the 30% sponge sample, with a plastic deformation of 50% (Table 2), after the first scan and a measured porosity of 60% (Table 1).

Conclusions

Films and sponges were prepared from a solution of Poly (ε-caprolactone) (PCL) in tetrahydrofuran (THF). The samples obtained by liquid phase separation (sponges) and by solvent casting technique (film) have higher crystallinity than the samples obtained by melting the PCL (bulk). The sponge porosity depends on the PCL concentration in the PCL/THF solution and ranges from 50% to 70%; the porosity of the film samples does not depend on the PCL concentration in the solution. The crystallinity in the film samples decreases when there is an increase in the PCL concentration, but the crystallinity of the sponges increases with PCL concentration.

The compression scans do not affect the crystallinity of the samples. The corresponding differences observed in the porous samples could be explained as an effect of the densification that produces the pore collapse, due to elastoplastic deformation. The unit strain at the end of the first scan is always greater than that corresponding to the same stress in the successive scans. This behavior could be correlated with a lateral expansion in the bulk sample and with plastic densification in the case of porous samples.

From the mechanical characterization it can be concluded that these porous PCL samples have the potential for applications in bone and cartilage tissue engineering. Future research projects include obtaining suitable surface chemistry for cell attachment, proliferation, and differentiation, with controllable degradation and resorption rates to match tissue replacement.

Acknowledgments This work was supported by the Spanish Science and Technology Ministry through the MAT2003-05391-C03-01 project. The support given to the research group by the Generalitat Valenciana through the GV04A/345 project, is also acknowledged. We would like to thank the R+D+i Linguistic Assistance Office at the Polytechnic University of Valencia for their help in revising this paper.

References

1. G. L. BRODE and J. V. KOLESKE, *J. Macromol. Sci. Chem.* **A6** (1972) 1109
2. Y. SONG, L. LIU, X. WENG and R. ZHUO, *J. Biomater. Sci. Polym. Ed*. **14** (2003) 241
3. H. W. KIM, J. C. KNOWLES and H. E. KIM, *J. Mater. Sci.: Mater. Med*. **16** (2005) 189
4. F. QUAGLIA, L. OSTACOLO, G. NESE, G. DE ROSA, M. LA ROTONDA, R. PALUMBO and G. MAGLIO, *Macromol. Biosci*. **5** (2005) 945
5. S. Y. CHEW, T. C. HUFNAGEL, C. T. LIM and K. W. LEONG, *Nanotechnology* **17** (2006) 3880
6. Z. K. ZHONG and X. Z. SUN, *Polymer* **42** (2001) 6961
7. H. Y. KWEON, M. K. YOO, I. K. PARK, T. H. KIM, H. C. LEE, H. S. LEE, J. S. OH, T. AKAIKE and C. S. CHO, *Biomaterials* **24** (2003) 801
8. S. L. ISHAUG-RILEY, L. E. OKUN, G. PRADO, M. A. APPLEGATE and A. RATCLIFFE, *Biomaterials* **20** (1999) 2245
9. G. CHEN, P. ZHOU, N. MEI, X. CHEN, Z. SHAO, L. PAN and C. WU, *J. Mater. Sci.: Mater. Med.* **15** (2004) 671
10. H. L. KHOR, K. W. NG, A. S. HTAY, J. T. SCHANTZ, S. H. TEOH and D. W. HUTMACHER, *J. Mater. Sci.: Mater. Med.* **14** (2003) 113
11. C. G. PITT, F. I. CHASALOW, Y. M. HIBIONADA, D. M. KLIMAS and A. SCHINDLER, *J. Appl. Polym. Sci*. **26** (1981) 3779
12. S. A. M. ALI, S. P. ZHONG, P. J. DOHERTY and D. F. WILLIAMS, *Biomaterials* **14** (1993) 648
13. V. R. SINHA, K. BANSAL, R. KAUSHIK, R. KUMRIA and A. TREHAN, *Int. J. Pharm.* **278** (2004) 1
14. H. SUN, L. MEI, C. SONG, X. CUI and P. WANG, *Biomaterials* **27** (2006) 1735
15. M. R. WILLIAMSON, E. F. ADAMS and A. G. A. COOMBES, *Biomaterials* **27** (2006) 1019
16. A. G. A. COOMBES, S. C. RIZZI, M. WILLIAMSON, J. E. BARRALET, S. DOWNES and W. A. WALLACE, *Biomaterials* **25** (2004) 315
17. W. LI, R. TULI, C. OKAFOR, A. DERFOUL, K. G. DANIELSON, D. J. HALL and R. S. TUAN, *Biomaterials* **26**, (2005) 599
18. T. J. CORDEN, I. A. JONES, C. D. RUDD, P. CHRISTIAN, S. DOWNES and K. E. MCDOUGALL, *Biomaterials* **21** (2000) 713
19. J. T. SCHANTZ, D. W. HUTMACHER, C. X. LAM, M. BRINKMANN, K. M. WONG, T. C. LIM, N. CHOU, R. E. GULDBERG and S. H. TEOH, *Tissue Eng.* **9**(Suppl 1) (2003) S127
20. M. D. BENDER, J. M. BENNET, R. L. WADDELL, J. S. DOCTOR and K. G. MARRA, *Biomaterials* **25** (2004) 1269
21. P. X. MA and J. W. CHOI, *Tissue Eng.* **7** (2001) 23
22. Z. MA, C. GAO, Y. GONG and J. SHEN, *Biomed. Mater. Res. Part B: Appl. Biomater.* **67B** (2003) 610
23. J. REIGNIER and M. HUNEAULT, *Polymer* **47** (2006) 4076
24. M. H. SHERIDAN, L. D. SHEA, M. C. PETERS and D. J. MOONEY, *J. Control. Release* **64** (2000) 91
25. A. G. MIKOS, Y. BAO, L. CIMA, D. INGBER, J. P. VACANTI and R. LANGER, *J. Biomed. Mater. Res.* **27** (1993) 183
26. M. MARIANI, F. ROSATINI, G. VOZZI, A. PREVITI and A. AHLUWALIA, *Tissue Eng.* **12** (2006) 547
27. D. W. HUTMACHER, T. SCHANTZ, I. ZEIN, K. W. NG, S. H. TEOH and K. C. TAN, *J. Biomed. Mater. Res*. **55** (2001) 203
28. F. YANG, R. MURUGAN, S. RAMAKRISHNA, X. WANG, Y. X. MA and S. WANG, *Biomaterials* **25** (2004) 1891
29. Z. G. TANG, R. A. BLACK, J. M. CURRAN, J. A. HUNT, N. P. RHODES and D. F. WILLIAMS, *Biomaterials* **25** (2004) 4741
30. S. J. HOLLISTER, R. D. MADDOX and J. M. TABOAS, *Biomaterials* **23** (2002) 4095
31. I. ENGELBERG and J. KHON, *Biomaterials* **12** (1991) 292
32. S. DUMITRIU, in "Polymeric Biomaterials" 2nd edn. (Marcel Dekker, New York, 2002) p. 95
33. L. GIBSON and M. ASHBY, in "Cellular Solids: Structure and Properties" (Cambridge University Press, Cambridge, 1997) chapter 5
34. L. E. NIELSEN, in "Mechanical Properties of Polymers and Composites" (Marcel Dekker, New York, 1974) vol. 1, chapter 2